Beamforming Design and Performance Analysis for Satellite and UAV Integrated Networks in IoRT Applications

This article has been accepted for publication in a future issue of this journal, but has not been fully edited. Content may change prior to final publication. Citation information: DOI 10.1109/JIOT.2022.3170429, IEEE Internet of Things Journal

Beamforming Design and Performance Analysis for Satellite and UAV Integrated Networks in IoRT Applications

Huaicong Kong, Min Lin, *Member, IEEE,* Jian Zhang, Jian Ouyang, *Member, IEEE,* Wei-Ping Zhu, *Senior Member, IEEE,* and Mohamed-Slim Alouini, *Fellow, IEEE*

***Abstract*—Satellite and unmanned aerial vehicles (UAV) integrated networks (SUINs) are considered as a promising method to offer various internet of remote things (IoRT) applications. In this paper, we investigate the downlink transmission of SUINs where the satellite to UAV link uses free-space optical (FSO) technology with equal gain combining (EGC) scheme while the links from UAV to IoRT devices exploit radio frequency (RF) with space division multiple access (SDMA) technique. Specifically, considering that only statistical channel state information (CSI) is available, we first formulate an optimization problem to maximize the ergodic sum rate (ESR) of the system, which is constrained by total transmit power budget and IoRT devices' rate requirements. Then, a beamforming (BF) scheme based on alternating direction method of multipliers (ADMM) is proposed to solve the non-convex problem. Furthermore, a zero-forcing (ZF) based suboptimal approach is also presented to reduce the implementation complexity. Finally, by assuming that the FSO link and RF links are subject to Gamma-Gamma fading and Nakagami-m fading, respectively, we derive closed-form ESR expressions for the considered network with the proposed BF schemes. Simulation results are provided to confirm the accuracy of theoretical analysis. Moreover, it is revealed that our proposed EGC scheme for FSO communication and BF schemes for RF transmission can both achieve better performance than the existing works.**

***Index Terms*—Satellite and UAV integrated networks, internet of remote things, statistical channel state information, ergodic sum rate, space division multiple access, alternating direction method of multipliers.**

I. Introduction

RECENTLY, internet of things (IoT) has been considered as one of the essential applications of the fifth generation (5G) and beyond wireless communications, since it can provide ubiquitous wireless connectivity for a large number of IoT devices and thus improve the quality of our daily life [1]-[3]. However, due to the limitation of geographical conditions and deployment expense, traditional terrestrial cellular networks are either unavailable or scarce for smart devices deployed in rural areas, hotspot areas, isolated areas and emergency areas. In this case, IoT networks are therefore referred to as internet of remote things (IoRT) networks [4], [5], in which smart devices cannot be served by existing terrestrial communications so that both the wireless coverage and quality-of-service (QoS) requirements become an outstanding issue. To solve this issue, as an effective complement and expansion of the ground communication networks, satellite communication (SatCom) has a great prospect to realize connection from anytime, anywhere, anyone, to anything in IoRT networks [6]. Based on the inherent characteristics of SatCom, satellites can not only fulfill the requirements of massive connections in IoRT networks, but also provide continuous communications in case of remote or disaster areas [7], [8]. Therefore, the application of SatCom in IoRT networks has drawn substantial global attention in the past few years, and has been widely investigated in open literature. For example, many scholars have made in-depth studies of typical scenarios of IoRT networks, such as smart grid, forest monitoring and emergency communication [6], [9].

Although IoRT networks based on SatCom have achieved major technique breakthroughs in both several unserved and under-served scenarios [6], such as providing a more cost-effective solution for connection and communication in remote areas as compared to other terrestrial technologies, many challenges are still faced. For example, the quality of satellite link is not guaranteed due to certain practical facts [9], such as masking effects and large path-loss. On the other hand, considering that smart devices are generally energy limited, and subject to low latency and short distance transmission [10], it is difficult to randomly access satellite networks for long time communications. In this context, using unmanned aerial vehicle (UAV) as an aerial relay is an effective approach to tackle the aforementioned challenges for IoRT networks [11]. With the help of UAV, the line-of-sight (LoS) communication links can be established in a flexible fashion. In addition, it is particularly suitable for on-demand emergency communication with fast deployment. From the prospective of IoRT networks, a UAV holds the potential to meet the massive access requirements of smart devices in remote areas, since it has the advantages of high mobility and low cost in favour of coverage expansion and overhead reduction of the IoRT networks. With this regard, integrating UAV into SatCom networks for IoRT scenarios can achieve large coverage and seamless connectivity, thereby enhancing the communication QoS of the increasingly

This work was supported by the Key International Cooperation Research Project under Grant 61720106003. (*Corresponding author: Min Lin.*)

H. Kong, M. Lin, J. Zhang and J. Ouyang are with the College of Telecommunications and Information Engineering, Nanjing University of Posts and Telecommunications, Nanjing 210003, China (e-mail: khc_dream@163.com, linmin@njupt.edu.cn, j_zhang_njupt@163.com, ouyangjian@njupt.edu.cn).

W.-P. Zhu is with the Department of Electrical and Computer Engineering, Concordia University, Montreal, QC H3G 1M8, Canada, and also with the College of Telecommunications and Information Engineering, Nanjing University of Posts and Telecommunications, Nanjing 210003, China (e-mail: weiping@ece.concordia.ca).

M.-S. Alouini is with the Computer, Electrical, and Mathematical Science and Engineering Division, King Abdullah University of Science and Technology, Thuwal 23955, Saudi Arabia (e-mail: slim.alouini@kaust.edu.sa).

This article has been accepted for publication in a future issue of this journal, but has not been fully edited. Content may change prior to final publication. Citation information: DOI 10.1109/JIOT.2022.3170429, IEEE Internet of Things Journal

prosperous IoRT networks [12], [13]. The novel architecture referred to as satellite and UAV integrated networks (SUIN) can break through the limitations of terrestrial cellular networks in terms of coverage area and network capacity. In particular, it can provide high data rate and reliable wireless communications in remote areas, as widely studied in many existing works such as [5], [14].

Furthermore, in SUIN for IoRT, satellite can provide UAVs with backbone connection to the internet through radio frequency (RF) link and has been well studied in under way projects, such as the Inmarsat and the Thuraya [14]. However, since the RF spectrum is more and more scarce, free-space optical (FSO) communication has emerged as an attractive complementary technology to RF with the explosive growth of smart devices and data traffic [15]. Moreover, FSO communication systems are free from interference and able to communicate over long distance, which has been applied in SatCom and UAV systems by license-free electromagnetic spectrum. To this end, a new SUIN with mixed FSO-RF channels is envisioned as a promising architecture to meet the requirement for the growing IoRT applications.

A. Related Works and Motivation

In 5G and beyond, IoRT becomes increasingly important to provide services for a large number of smart devices outside the coverage of current cellular networks. Among other techniques, satellite integrated 5G IoRT network has been introduced to provide service continuity for various smart devices in remote or sparsely populated areas [16], [17]. From the power perspective, the authors of [18] conducted some link budget analysis to prove that the direct access is possible at the cost of a significant decrease of the achievable data rate due to large latency. In [6], the authors pointed out that spectrum efficiency is a huge bottleneck in satellite IoRT networks. From these works, the direct access from satellite to smart devices is not a viable option, when taking into account low-cost and low-energy-consumption IoRT devices [19]. Therefore, UAV systems as another choice to support massive access for smart devices in IoRT scenarios have attracted more interest in academia. For example, in [20], the authors derived analytical expressions for outage probability and ergodic rate to measure the performance of the 3-D UAV system. In [21], the authors investigated the throughput maximization problem constrained by transmitted power, UAV trajectory and practical mobility. The authors of [22] studied a UAV-assisted network and proposed a new cooperative interference cancellation scheme, which aims to eliminate the co-channel interference while maximize the sum-rate achievable by the ground base stations. Besides, the authors of [11] illustrated a very comprehensive overview of the utilization of UAVs and their role in an integrated 5G network. The existing related works in [23], [24] and [25] conducted the performance analysis for a satellite-aerial-terrestrial network with decode-and-forward (DF) protocol and amplify-and-forward (AF) protocol, respectively. It is worth mentioning that, most of previous works have assumed that the channel state information (CSI) is perfectly known, which is impossible for UAV-assisted IoT systems due to the energy limitation and estimation error.

Moreover, the authors of [26] proposed a two-layer UAV communication system, in which the lower-layer is employed to transmit with ground smart devices and the upper-layer is used as fusion center. This work mainly focused on a smart city IoT scenario that is different from the considered SUIN for IoRT cases in our work, where the channel capacity and large connectivity of IoRT networks can be improved significantly relying on such integrated networks. Similar research topics on SUIN have been widely investigated in [5], [14], where the satellite-to-UAV transmission is via a RF link. Recently, FSO communication has been regarded as an attractive candidate to RF with the exponentially increasing growth of smart devices [15], [27]. Moreover, FSO communication systems are free from interference due to their narrow beams and are able to communicate over long distances with lower power consumption, which has been applied between satellite and UAV [28], [29] and even between satellite and gateway [30], [31]. In particular, the authors in [28] showed feasibility of the FSO link in satellite-to-UAV communication by an interesting and fascinating experiment. Accordingly, FSO technology is very suitable for the large capacity connections in the considered satellite and UAV integrated networks. Under this situation, mixed FSO/RF transmission has received significant attention in recent years. For instance, the performance analysis of a satellite-terrestrial FSO cooperative network was conducted in [32] for AF protocol and in [33] for DF protocol. In [34], the authors investigated the performance of the mixed FSO/RF channels in a multiuser system with opportunistic scheduling. Besides, the authors of [35] analyzed outage probability, average bit error rate and ergodic capacity of the multiuser mixed FSO/RF network with fixed-gain and variable gain AF protocols. The above works [34], [35] were quite limited to single antenna RF transmission in mixed FSO/RF networks with multiple users. This has led to the concept of multiple antennas technique applied in RF links to provide a reliable transmission with remarkable increasing achievable rate [36]-[39]. Specifically, the authors of [36] analyzed the ergodic sum rate (ESR) of the UAV-based communication network where a FSO backhaul link connecting to optical ground station (OGS) is considered. This investigation is very interesting, but the focus is on a limited area case, which is rather overoptimistic for practical scenario where no terrestrial internet connectivity is available. In this context, the authors of [37]-[39] extened the mixed FSO-RF transmission in satellite and UAV integrated networks for IoRT applications, where the backbone connection between satellite and UAV is through FSO technology to provide high-capapcity link. In addition, future communication system should support massive access for a large number of smart devices in remote rural areas. Therefore, in recent years, multi-antenna and beamforming (BF) technologies are often used to improve the system performance and QoS requirements [16], however, BF design therein is based on the assumption of accurate known CSI. When UAV is equipped with a massive antenna array, the amount of feedback

This article has been accepted for publication in a future issue of this journal, but has not been fully edited. Content may change prior to final publication. Citation information: DOI 10.1109/JIOT.2022.3170429, IEEE Internet of Things Journal

required for estimation increases sharply, and the energy of the UAV is always limited. Therefore, there is an urgent need for a novel array signal processing (ASP) technique that can provide superior performance for the scenario where the perfect CSI is unavailable.

B. Our Contribution

Motivated by the above observations, we here investigate the downlink transmission of a satellite and UAV integrated network in IoRT applications. Specifically, the contributions of this paper can be summarized as follows:

- First, we consider the framework of mixed FSO-RF transmission in a satellite and UAV integrated network to meet the increasing demands for IoRT devices. Here, equal gain combining (EGC) scheme is adopted for FSO transmission to achieve higher data rate than that of works [37]-[39] where the optical receiver is equipped with a single aperture. As for the RF communication, space division multiple access (SDMA) technique is exploited to improve spectrum utilization, which is more general and efficient compared with [37], [39] employing multiuser scheduling in RF links.
- Next, by assuming that the statistical CSI is available at the UAV, we aim at maximizing the ergodic sum rate (ESR) under the constraints of total transmit power and QoS requirement of each IoRT device. We propose a BF scheme using alternating direction method of multipliers (ADMM) to solve the non-convex problem. Further, to reduce the algorithm complexity, we propose a zero-forcing (ZF) based suboptimal scheme and obtain its closed-form solution. Our proposed BF schemes are more practical than the previous works [23], [24] which rely on perfect CSI at the UAV to conduct BF design.
- Finally, by considering that FSO links follow Gamma-Gamma fading while RF links undergo Nakagami-m fading, we derive closed-form expression for the ESR of the considered system with buffer-aided DF protocol. Unlike the work [27] that considers only one user and the RF channel modeled as Rayleigh distribution, we here deal with a more general performance analysis of multiuser satellite and UAV integrated networks with mixed FSO-RF channels. Numerical examples validated by simulations are presented to show the effectiveness of the proposed schemes and the performance analysis.

C. Paper Organization and Notation

The rest of this paper is organized as follows. Section II introduces the system model and formulates the ESR maximization problem. Then, BF schemes based on statistical CSI are proposed in Section III. In Section IV, we describe statistical characteristics of channel links and derive accurate analytical expressions for ESR of the considered network with the proposed BF schemes. Section V provides simulation results and discussions. Finally, conclusions of this paper are drawn in Section VI.

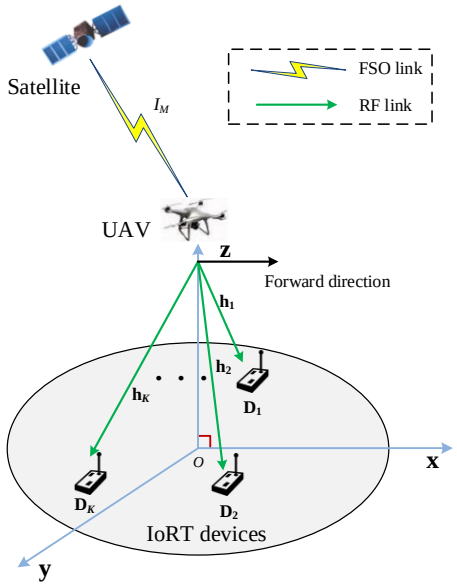

Fig. 1. System model of the considered network

Notations: Matrices and vectors are denoted by bold upper-case and lower-case letters, respectively. $E[\cdot]$ represents the expectation, $(\cdot)^H$ the Hermitian transpose, $|\cdot|$ the absolute value, $\|\cdot\|$ the Euclidean norm of a vector, $\frac{df(x)}{dx}$ denotes derivative operator, and $\mathbf{I}_N$ the $N \times N$ identity matrix. Besides, $\mathbb{C}^{M\times N}$ stands for the complex space of $M \times N$ and $[\cdot]^+ \triangleq \max(\cdot, 0)$. $G_{p,q}^{m,n}[\cdot|\cdot]$ and $\Gamma(\cdot)$ represent the Meijers G-function and the Gamma function, respectively.

II. System Model and Problem Formulation

In this section, we first introduce the system model for the considered satellite and UAV integrated network facilitating downlink transmission between a GEO satellite and IoRT devices. Then, we formulate an optimization problem to maximize the ergodic sum rate subject to the constraints of total power budget and the requirement for each IoRT device.

A. System Model

As illustrated in Fig. 1, we consider the downlink transmission of a satellite and UAV integrated network for IoRT applications, which consists of a GEO satellite, a rotary-wing UAV hovering in the sky[1] and many IoRT devices on the ground. Unlike most of the existing works [5], [14], it is assumed here that FSO technology is adopted over satellite-to-UAV link to take the advantages of its unlicensed spectrum resource, being free from interference and high security, while RF communication is employed over UAV-to-device links with UAV having multi-antenna and conducting SDMA to improve the spectrum efficiency. In addition, the UAV is equipped with M receive apertures for collecting the received optical signal from the satellite and N-element uniform linear array (ULA) to

[1]Here, the UAV with superior hardware resource can provide data receiving, processing, and transmitting functionalities to serve as aerial relay between satellite and ground devices [11].

implement BF so that K ($K \leqslant N$) single-antenna IoRT devices on the ground can be served simultaneously.

The overall downlink transmission can be accomplished over two phases. In the first phase, the GEO satellite utilizes wavelength-division multiplex (WDM) technique to multiplex the optical carriers into a single mode fiber, and then sends optical signal through the telescope towards the UAV. At the UAV, the optical signal from satellite is captured by the telescope and combined with M apertures, then de-multiplexed to separate the individual WDM channels, converted to electrical signals and thereby serving ground IoRT devices [31]. Hence, the received electrical RF signal at the q-th aperture of UAV is given by

$$y_q = \sqrt{P_1}\eta I_q x_s + n_q, q = 1, 2, \cdots, M, \tag{1}$$

where x_s is the intensity modulated optical signal, P_1 is the transmit power at satellite, η is the optical-to-electrical conversion coefficient, and n_q is additive white Gaussian noise (AWGN) with zero mean and variance N_0 [31]. Besides, the term I_q in (1) denotes the scalar fading coefficient that models the atmospheric turbulence through the FSO channel, which is assumed to be independent and identically distributed (i.i.d). To mitigate the atmosphere turbulence in FSO links, we employ EGC scheme where the signal on each aperture is added with equal weight. Here, we prefer EGC over maximal ratio combining because both have comparable performance, but EGC does not require CSI. Thus, the output electrical SNR of combined signal at the UAV can be expressed as

$$\gamma_1 = \frac{P_1 \eta^2 I_{EGC}^2}{M N_0} \triangleq \bar{\gamma}_1 I_{EGC}^2, \tag{2}$$

where $I_{EGC} = \sum_{q=1}^{M} I_q$ and $\bar{\gamma}_1 = \frac{P_1 \eta^2}{M N_0}$ is the average SNR.

In the second phase, when the DF protocol is adopted, the UAV forwards the recoded signal $x_i, i = 1, \cdots, K$ with $E\left[|x_i|^2\right] = 1$ to IoRT device through the RF channels. In order to implement SDMA, transmit BF with normalized weight vector $\mathbf{w} \in \mathbb{C}^{N \times 1}$ is employed at the UAV for RF transmission, leading to the received signal at the IoRT device D_i given by

$$y_{2,i} = \sqrt{P_{2,i}}\mathbf{h}_i^H \mathbf{w}_i x_i + \sum_{j=1, j\neq i}^{K} \sqrt{P_{2,j}}\mathbf{h}_i^H \mathbf{w}_j x_j + n_{2,i}, \tag{3}$$

As a result, the expression for instantaneous signal-to-interference-and-noise ratio (SINR) $\tilde{\gamma}_{2,i}$ at the IoRT device D_i reads as

$$\tilde{\gamma}_{2,i} = \frac{P_{2,i}\left|\mathbf{h}_i^H \mathbf{w}_i\right|^2}{\sum_{j=1, j\neq i}^{K} P_{2,j}\left|\mathbf{h}_i^H \mathbf{w}_j\right|^2 + \sigma_i^2}, \tag{4}$$

where $P_{2,i}$ denotes the transmit power of UAV to IoRT device D_i, and $\mathbf{h}_i$ the RF channel vector. In (3), $n_{2,i}$ is the AWGN with zero-mean and variance σ_i^2.

Here, we adopt buffer technology for DF protocol at UAV, which can select the best strategy based on the channel conditions for FSO and RF links to enhance the end-to-end achievable sum rate [36]. To this end, the system ergodic sum rate can be expressed as

$$R = \min\left(R_1, R_2\right). \tag{5}$$

Using (2), the ergodic rate R_1 for FSO link is given by [36]

$$R_1 = B_o E\left[\log_2\left(1+\gamma_1\right)\right] = B_o E\left[\log_2\left(1+\bar{\gamma}_1 I_{EGC}^2\right)\right], \tag{6}$$

where B_o is the bandwidth of FSO link. The ergodic sum rate R_2 in (5) for RF links can be obtained as [36]

$$R_2 = B_R \sum_{i=1}^{K} R_i = B_R \sum_{i=1}^{K} E\left[\log_2\left(1+\tilde{\gamma}_{2,i}\right)\right]. \tag{7}$$

where B_R is the bandwidth of RF transmission. Correspondingly, substituting (4) into (7), the ergodic rate R_i for the IoRT device D_i in RF transmission is denoted by

$$R_i = E\left[\log_2\left(1 + \frac{P_{2,i}\left|\mathbf{h}_i^H \mathbf{w}_i\right|^2}{\sum_{j=1, j\neq i}^{K} P_{2,j}\left|\mathbf{h}_i^H \mathbf{w}_j\right|^2 + \sigma_i^2}\right)\right]. \tag{8}$$

B. Channel Models

In the considered system model, FSO is a promising technology for satellite-to-UAV link to achieve ultrahigh capacity and high reliable transmission. Unlike the existing works using a single aperture at the optical receiver [37]-[39], UAV is equipped with M receive apertures. Then, similar to [30], [37], the q-th FSO channel can be mathematically modeled as

$$I_q = I_l I_a, \tag{9}$$

where $I_l = \frac{1}{2}\left(G_t + G_r - A_{FS} - A_{Atm} - L - M_s\right)$ [dB] with $G_t, G_r, A_{FS}, A_{Atm}, L$ and M_s being, respectively, transmitter gain, receiver gain, free space loss, atmosphere attention, lenses losses, and system margin [37]. Besides, for the fading parameter I_a of FSO link with atmospheric turbulence, Gamma-Gamma distribution is preferred commonly due to its suitability to consider both the large and small scale atmospheric fluctuations [37]-[39]. With this regard, the PDF of I_a is given by

$$f_{I_a}(x) = \frac{2(\alpha\beta)^{\frac{\alpha+\beta}{2}} x^{\frac{\alpha+\beta}{2}-1}}{\Gamma(\alpha)\Gamma(\beta)} K_{\alpha-\beta}\left(2\sqrt{\alpha\beta x}\right), x \geqslant 0, \tag{10}$$

where α and β denote the parameters related to the atmospheric turbulence conditions. They can be derived by

$$\alpha = \left\{\exp\left[\frac{0.49\sigma_R^2}{\left(1+1.11\sigma_R^{12/5}\right)^{7/6}}\right] - 1\right\}^{-1}, \tag{11}$$

$$\beta = \left\{\exp\left[\frac{0.51\sigma_R^2}{\left(1+0.69\sigma_R^{12/5}\right)^{5/6}}\right] - 1\right\}^{-1}, \tag{12}$$

This article has been accepted for publication in a future issue of this journal, but has not been fully edited. Content may change prior to final publication. Citation information: DOI 10.1109/JIOT.2022.3170429, IEEE Internet of Things Journal

where σ_R^2 is Rytov variance, which is termed as a metric of the strength of turbulence fluctuations. With the help of [40], (10) can be denoted in terms of Meijer's G-function as

$$f_{I_a}(x) = \frac{(\alpha\beta)^{\frac{\alpha+\beta}{2}} x^{\frac{\alpha+\beta}{2}-1}}{\Gamma(\alpha)\Gamma(\beta)} G_{0,2}^{2,0}\left[\alpha\beta x \middle| \begin{matrix} - \\ \frac{\alpha-\beta}{2}, -\frac{\alpha-\beta}{2} \end{matrix}\right], x \geqslant 0. \tag{13}$$

The combined channel state PDF accounting for both atmospheric turbulence and other loss is obtained as

$$f_{I_q}(x) = \left|\frac{d}{dI_q}\left(\frac{I_q}{I_l}\right)\right| f_{I_a}\left(\frac{I_q}{I_l}\right). \tag{14}$$

Hence, the PDF of I_q can be expressed as

$$f_{I_q}(x) = \frac{(\alpha\beta)^{\frac{\alpha+\beta}{2}} x^{\frac{\alpha+\beta}{2}-1}}{\Gamma(\alpha)\Gamma(\beta) I_l^{\frac{\alpha+\beta}{2}}} G_{0,2}^{2,0}\left[\frac{\alpha\beta x}{I_l} \middle| \begin{matrix} - \\ \frac{\alpha-\beta}{2}, -\frac{\alpha-\beta}{2} \end{matrix}\right], x \geqslant 0. \tag{15}$$

To visually obtain the position and geometry relationship of the UAV and IoRT devices, a three-dimensional Cartesian coordinate system is established, as presented in Fig. 1, where the UAV flies at a fixed location with coordinate $(0,0,\mathrm{H})$ and IoRT devices are uniformly distributed on the horizontal plane with coordinates $(x_i, y_i, 0)$, $i = 1, 2, \cdots, K$. Then, the channel vectors $\mathbf{h}_i$ in realistic UAV RF links can be described by Nakagami-m fading [2] combined with antenna pattern and path loss, which can be expressed as

$$\mathbf{h}_i = \ell_i \mathbf{g}_i, \tag{16}$$

where ℓ_i in dB is given by [8], [42]

$$\ell_i = \frac{1}{2}\left(10\alpha_l \log d_i + 20\log f + 92.4\right), \tag{17}$$

with α_l denoting the path loss exponent depends on the environment, f in GHz being carrier frequency, and d_i in km being the distance between UAV and the IoRT device D_i as given by

$$d_i = \sqrt{x_i^2 + y_i^2 + \mathrm{H}^2}. \tag{18}$$

Besides, the channel fading vector $\mathbf{g}_i$ in (16) can be denoted as

$$\mathbf{g}_i = \rho_i \mathbf{a}(\theta_i), \tag{19}$$

where ρ_i is a random variable obeying Nakagami-m distribution with average power Ω_i and severity parameter m_i, i.e., $|\rho_i| \sim \text{Nakagami}(m_i, \Omega_i)$, which is given as [36], [41]

$$f_{|\rho_i|^2}(x) = \frac{m_i^{m_i} x^{m_i-1}}{\Omega_i^{m_i}\Gamma(m_i)} \exp\left(-\frac{m_i x}{\Omega_i}\right). \tag{20}$$

For ULA structure, the array steering vector $\mathbf{a}(\theta_i)$ in (19) is given by

$$\mathbf{a}(\theta_i) = \left[1, e^{j\kappa d_a \cos\theta_i}, \cdots, e^{j(N-1)\kappa d_a \cos\theta_i}\right]^T, \tag{21}$$

[2]As described in Section III-B of [41], Nakagami$m$ fading distribution can offer substantial flexibility to study the UAV-to-ground fading channel characteristics in mobile and fixed scenarios. Therefore, we here use the Nakagami-m channels to model the aerial-terrestrial RF links.

where $\kappa = 2\pi/\lambda$ denotes the wavenumber, d_a the antenna element spacing along ULA, and θ_i the angle-of-departure (AoD) from the UAV to the IoRT device D_i, being expressed as

$$\begin{aligned}\theta_i &= \arccos\left\{\frac{[x_i, y_i, -\mathrm{H}]\cdot[1,0,0]}{|[x_i, y_i, -\mathrm{H}]| \times |[1,0,0]|}\right\} \\ &= \frac{x_i}{\sqrt{x_i^2 + y_i^2 + \mathrm{H}^2}},\end{aligned} \tag{22}$$

where $\mathbf{a}\cdot\mathbf{b}$ denotes dot product and $[1,0,0]$ is the forward direction vector. In the following, we will formulate an optimization problem to be solved in this paper based on the considered system model.

C. Problem Formulation

It is an immediate and basic problem to maximize the system ergodic sum rate under the condition that total transmit power is constrained, while guaranteeing the requirement of each IoRT device for the considered network. With respect to (5), we find that R_1 and R_2 are independent of each other and hence, the whole mixed FSO-RF network can be regarded as two independent subsystems without performance loss. In this context, we focus on ESR maximization problem for RF transmission and it can be separately formulated as

$$\max_{\mathbf{w}_i, P_{2,i}} R_2 \tag{23a}$$

$$\text{s.t. } E\left[\text{SINR}_i\right] \geqslant \gamma_{th}, \forall i = 1, \cdots, K, \tag{23b}$$

$$\sum_{i=1}^{K} P_{2,i} \leqslant P_2^{\max}, \tag{23c}$$

$$\mathbf{w}_i^H \mathbf{w}_i = 1. \tag{23d}$$

where $P_2^{\max}$ denotes the maximal transmit power of the UAV. Note that the constraint (23c) considers the limited battery of the UAV. Besides, the constraint $E\left[\text{SINR}_i\right] \geqslant \gamma_{th}, \forall i = 1, \cdots, K$ is denoted by

$$E\left[\text{SINR}_i\right] = E\left[\frac{P_{2,i}\left|\mathbf{h}_i^H \mathbf{w}_i\right|^2}{\sum\limits_{j=1, j\neq i}^{K} P_{2,j}\left|\mathbf{h}_i^H \mathbf{w}_j\right|^2 + \sigma_i^2}\right] \geqslant \gamma_{th}, \forall i = 1, \cdots, K \tag{24}$$

where γ_{th} is the SINR threshold. Then, the optimization problem for maximizing R_2 can be described as

$$\begin{aligned} &\max_{\mathbf{w}_i, P_{2,i}} \quad R_2 \\ &\text{s.t. } E\left[\frac{P_{2,i}\left|\mathbf{h}_i^H \mathbf{w}_i\right|^2}{\sum\limits_{j=1, j\neq i}^{K} P_{2,j}\left|\mathbf{h}_i^H \mathbf{w}_j\right|^2 + \sigma_i^2}\right] \geqslant \gamma_{th}, \forall i = 1, \cdots, K, \\ &\quad \sum_{i=1}^{K} P_{2,i} \leqslant P_2^{\max}, \\ &\quad \mathbf{w}_i^H \mathbf{w}_i = 1. \end{aligned} \tag{25}$$

Note that the constrained optimization problem (25) is interesting yet challenging, not only due to the non-convex objective

This article has been accepted for publication in a future issue of this journal, but has not been fully edited. Content may change prior to final publication. Citation information: DOI 10.1109/JIOT.2022.3170429, IEEE Internet of Things Journal

function, but also the parameters to be optimized are entangled with each other. In the following, we will propose two different BF schemes to solve the ESR maximization problem for RF transmission in our considered satellite and UAV integrated networks.

III. Proposed BF Schemes

By assuming the availability of statistical CSI (SCSI) rather than perfect CSI in practical UAV communication, this section first proposes an ADMM based BF scheme to solve the non-convex problem (25) for RF transmission. Further, to reduce the implementation complexity, we propose a ZF based suboptimal BF scheme and obtain its closed-form solution. Clearly, the analytical expression of R_2 makes (25) mathematically intractable. By adopting the Jensen's inequality, we can obtain an upper bound of R_2 as $R_2 = \sum_{i=1}^{K} R_i = \sum_{i=1}^{K} \log_2\left(1+E\left[\tilde{\gamma}_{2,i}\right]\right)$. Using (4) and Mullen's inequality, the optimization problem (25) can be reformulated as

$$\max_{\mathbf{w}_i, P_{2,i}} \; R_2 = \sum_{i=1}^{K} \log_2\left(1+\frac{P_{2,i}\mu_i \mathbf{w}_i^H \mathbf{A}_i \mathbf{w}_i}{\sum_{j=1, j\neq i}^{K} P_{2,j}\mu_i \mathbf{w}_j^H \mathbf{A}_i \mathbf{w}_j + 1}\right) \tag{26a}$$

$$\text{s.t.} \; \frac{P_{2,i}\mu_i \mathbf{w}_i^H \mathbf{A}_i \mathbf{w}_i}{\sum_{j=1, j\neq i}^{K} P_{2,j}\mu_i \mathbf{w}_j^H \mathbf{A}_i \mathbf{w}_j + 1} \geqslant \gamma_{th}, \forall i = 1, \cdots, K, \tag{26b}$$

$$\sum_{i=1}^{K} P_{2,i} \leqslant P_2^{\max}, \tag{26c}$$

$$\mathbf{w}_i^H \mathbf{w}_i = 1. \tag{26d}$$

where $\mu_i = \frac{\ell_i^2}{\sigma_i^2}$ and $\mathbf{A}_i \triangleq E\left[\mathbf{g}_i \mathbf{g}_i^H\right] = \Omega_i \mathbf{a}(\theta_i)\mathbf{a}(\theta_i)^H$ with $\Omega_i = E\left[|\rho_i|^2\right]$ denoting the covariance of the RF channels. For the sake of simplicity, we here omit the bandwidth of RF transmission, but it does not affect the solution of the optimzation problem. Obviously, the above problem still belongs to NP-hard, which is mathematically intractable. To overcome this difficulty, we will introduce a new SCSI-based BF scheme with ADMM method in the following subsection.

A. SCSI-Based ADMM BF Scheme

By denoting $\tilde{\mathbf{w}}_i = \sqrt{P_{2,i}}\mathbf{w}_i$, the original constrained optimization problem in (26) can be rewritten as

$$\max_{\tilde{\mathbf{w}}_1, \cdots, \tilde{\mathbf{w}}_K} \; \sum_{i=1}^{K} \log_2\left(1+\frac{\mu_i \tilde{\mathbf{w}}_i^H \mathbf{A}_i \tilde{\mathbf{w}}_i}{\sum_{j\neq i}^{K} \mu_i \tilde{\mathbf{w}}_j^H \mathbf{A}_i \tilde{\mathbf{w}}_j + 1}\right) \tag{27a}$$

$$\text{s.t.} \; \frac{\mu_i \tilde{\mathbf{w}}_i^H \mathbf{A}_i \tilde{\mathbf{w}}_i}{\sum_{j=1, j\neq i}^{K} \mu_i \tilde{\mathbf{w}}_j^H \mathbf{A}_i \tilde{\mathbf{w}}_j + 1} \geqslant \gamma_{th}, \forall i = 1, \cdots, K, \tag{27b}$$

$$\sum_{i=1}^{K} \|\tilde{\mathbf{w}}_i\|^2 \leqslant P_2^{\max}, \forall i = 1, \cdots, K, \tag{27c}$$

where $\mu_i \tilde{\mathbf{w}}_j^H \mathbf{A}_i \tilde{\mathbf{w}}_j$ denotes the interference terms. Here, we define $\varepsilon_{ij} = \mu_i \tilde{\mathbf{w}}_j^H \mathbf{A}_i \tilde{\mathbf{w}}_j$ and $B_i = \frac{1}{\sum_{j\neq i} \varepsilon_{ij}+1}$, then the problem (27) can be written as

$$\max_{\tilde{\mathbf{w}}_1, \cdots, \tilde{\mathbf{w}}_K} \; \sum_{i=1}^{K} \log_2\left(1+B_i \mu_i \tilde{\mathbf{w}}_i^H \mathbf{A}_i \tilde{\mathbf{w}}_i\right) \tag{28a}$$

$$\text{s.t.} \; \mu_i \tilde{\mathbf{w}}_i^H \mathbf{A}_i \tilde{\mathbf{w}}_i \geqslant \frac{\gamma_{th}}{B_i}, \forall i = 1, \cdots, K, \tag{28b}$$

$$\mu_i \tilde{\mathbf{w}}_j^H \mathbf{A}_i \tilde{\mathbf{w}}_j = \varepsilon_{ij}, \forall i, i \neq j, \tag{28c}$$

$$\sum_{i=1}^{K} \|\tilde{\mathbf{w}}_i\|^2 \leqslant P_2^{\max}, \forall i = 1, \cdots, K. \tag{28d}$$

After some mathematical manipulations, problem (28) can be reconstructed as

$$\max_{\mathbf{v}} \; \sum_{i=1}^{K} \log_2\left(1+B_i \mu_i \mathbf{v}^H \tilde{\mathbf{A}}_{ii} \mathbf{v}\right) \tag{29a}$$

$$\text{s.t.} \; \mu_i \mathbf{v}^H \tilde{\mathbf{A}}_{ii} \mathbf{v} \geqslant \frac{\gamma_{th}}{B_i}, \forall i = 1, \cdots, K, \tag{29b}$$

$$\mu_i \mathbf{v}^H \tilde{\mathbf{A}}_{ij} \mathbf{v} = \varepsilon_{ij}, \forall i, i \neq j, \tag{29c}$$

$$\mathbf{v}^H \mathbf{v} \leqslant P_2^{\max}, \tag{29d}$$

where $\mathbf{v} = \left(\tilde{\mathbf{w}}_1^T, \cdots, \tilde{\mathbf{w}}_K^T\right)^T$ and $\tilde{\mathbf{A}}_{il} = diag\left(0, \cdots, \mathbf{A}_i, \cdots, 0\right)$ with $\tilde{\mathbf{A}}_{il} (l \triangleq i, j)$ being a zeros block matrix whose l-th diagonal block element is equal to $\mathbf{A}_i$. It is obvious that problem (29) is a typical non-convex optimization problem and has been proven to be NP-hard. In the following, we will exploit a non-convex ADMM method [43] to solve problem (29). As a first step, we introduce a slack variable $\mathbf{x} \in \mathbb{C}^{N\times 1}$ and transform problem (29) into the following form

$$\min_{\mathbf{v}, \mathbf{x}} \; -\sum_{i=1}^{K} \log_2\left(1+B_i \mu_i \mathbf{v}^H \tilde{\mathbf{A}}_{ii} \mathbf{v}\right) \tag{30a}$$

$$\text{s.t.} \; \mu_i \mathbf{x}^H \tilde{\mathbf{A}}_{ii} \mathbf{x} \geqslant \frac{\gamma_{th}}{B_i}, \forall i = 1, \cdots, K, \tag{30b}$$

$$\mu_i \mathbf{x}^H \tilde{\mathbf{A}}_{ij} \mathbf{x} = \varepsilon_{ij}, \forall i, i \neq j, \tag{30c}$$

$$\mathbf{x}^H \mathbf{x} \leqslant P_2^{\max}, \tag{30d}$$

$$\mathbf{x} = \mathbf{v}. \tag{30e}$$

The augmented Lagrangian of problem (30) states

$$\begin{aligned} L(\mathbf{x}, \mathbf{v}, \lambda) = &-\sum_{i=1}^{K} \log_2\left(1+B_i \mu_i \mathbf{v}^H \tilde{\mathbf{A}}_i i \mathbf{v}\right) \\ &+ \lambda^H (\mathbf{v}-\mathbf{x}) + \frac{\rho}{2}\|\mathbf{v}-\mathbf{x}\|^2, \end{aligned} \tag{31}$$

where $\rho > 0$ is a penalty factor and $\lambda \in \mathbb{C}^N$ is Lagrangian multiplier. The ADMM method cyclically takes the following steps

$$\mathbf{x}^{t+1} \leftarrow \min_{\tilde{\mathbf{x}}} \left(\lambda^t\right)^H \left(\mathbf{v}^t - \tilde{\mathbf{x}}\right) + \frac{\rho}{2}\left\|\mathbf{v}^t - \tilde{\mathbf{x}}\right\|^2 \tag{32a}$$

$$\text{s.t.} \; \mu_i \tilde{\mathbf{x}}^H \tilde{\mathbf{A}}_i \tilde{\mathbf{x}} \geqslant \frac{\gamma_{th}}{B_i}, \forall i = 1, \cdots, K, \tag{32b}$$

$$\mu_i \tilde{\mathbf{x}}^H \tilde{\mathbf{A}}_{ij} \tilde{\mathbf{x}} = \varepsilon_{ij}, \forall i, i \neq j, \tag{32c}$$

$$\tilde{\mathbf{x}}^H \tilde{\mathbf{x}} \leqslant P_2^{\max}. \tag{32d}$$

This article has been accepted for publication in a future issue of this journal, but has not been fully edited. Content may change prior to final publication. Citation information: DOI 10.1109/JIOT.2022.3170429, IEEE Internet of Things Journal

$$\mathbf{v}^{t+1} \leftarrow \arg\min_{\mathbf{v}} \nabla\phi\left(\mathbf{x}^{t+1}\right)^H \left(\mathbf{v}-\mathbf{x}^{t+1}\right) + \lambda^H\left(\mathbf{v}-\mathbf{x}^{t+1}\right) + \frac{\rho+L}{2}\left\|\mathbf{v}-\mathbf{x}^{t+1}\right\|^2 \tag{33}$$

$$\lambda^{t+1} \leftarrow \lambda^t + \rho\left(\mathbf{v}^{t+1}-\mathbf{x}^{t+1}\right) \tag{34}$$

where $\phi(\mathbf{x}) = -\sum_{i=1}^{K}\log_2\left(1+B_i\mu_i\mathbf{x}^H\tilde{\mathbf{A}}_i\mathbf{x}\right)$, L is a constant greater than zero and satisfies $\|\nabla\phi(\mathbf{x}_1)-\nabla\phi(\mathbf{x}_2)\| \leqslant L\|\mathbf{x}_1-\mathbf{x}_2\|, \forall \mathbf{x}_1,\mathbf{x}_2$. Since the sub-problem (32) is relatively complex, we will focus on solving it later. The sub-problem (33) is equivalent to

$$\min_{\mathbf{v}} \left\|\mathbf{v}-\mathbf{x}^{t+1}+\frac{\nabla\phi\left(\mathbf{x}^{t+1}\right)+\lambda}{\rho+L}\right\|^2 \tag{35}$$

which has the closed-form solution

$$\mathbf{v}^{t+1} = \mathbf{x}^{t+1} - \frac{\nabla\phi\left(\mathbf{x}^{t+1}\right)+\lambda}{\rho+L} \tag{36}$$

Now, for the sub-problem (32), different from the commonly used semi-definite programming (SDP) algorithm in [7], we here adopt a consensus-ADMM method to solve it. By introducing K^2+1 variables $\tilde{\mathbf{x}}_k \in \mathbb{C}^{N\times 1},\ k \in \left\{1,\cdots,K^2+1\right\}$ into the sub-problem (32), it can be rewritten as

$$\tilde{\mathbf{x}}^{t+1} \leftarrow \arg\min_{\tilde{\mathbf{x}}} -\left(\lambda^t\right)^H\tilde{\mathbf{x}} + \frac{\rho}{2}\left\|\mathbf{v}^t-\tilde{\mathbf{x}}\right\|^2 \tag{37a}$$

$$\text{s.t. } \mu_i\tilde{\mathbf{x}}_k^H\tilde{\mathbf{A}}_i\tilde{\mathbf{x}}_k \geqslant \frac{\gamma_{th}}{B_i}, k=1,\cdots,K, \tag{37b}$$

$$\mu_i\tilde{\mathbf{x}}_k^H\tilde{\mathbf{A}}_{ij}\tilde{\mathbf{x}}_k = \varepsilon_{ij}, k=K+1,\cdots,K^2, \tag{37c}$$

$$\tilde{\mathbf{x}}_{K^2+1}^H\tilde{\mathbf{x}}_{K^2+1} \leqslant P_2^{\max}, \tag{37d}$$

$$\tilde{\mathbf{x}}_i = \tilde{\mathbf{x}}, k=1,\cdots,K^2+1. \tag{37e}$$

The augmented Lagrangian of problem (37) reads

$$L(\tilde{\mathbf{x}},\tilde{\mathbf{x}}_k,\lambda_k) = \frac{\rho}{2}\left\|\tilde{\mathbf{x}}-\mathbf{v}^t\right\|^2 - \left(\lambda^t\right)^H\tilde{\mathbf{x}} + \sum_{k=1}^{K^2+1}\lambda_k^H\left(\tilde{\mathbf{x}}-\tilde{\mathbf{x}}_k\right) + \sum_{k=1}^{K^2+1}\frac{\rho_k}{2}\|\tilde{\mathbf{x}}-\tilde{\mathbf{x}}_k\|^2. \tag{38}$$

Thus, the sub-problem (32) can be replaced by the following form

$$\tilde{\mathbf{x}}^{l+1} \leftarrow \frac{\sum_{k=1}^{K^2+1}\left(\rho_k\tilde{\mathbf{x}}_k^l-\lambda_k^l\right)+\lambda^t}{\rho+\sum_{k=1}^{K^2+1}\rho_k} \tag{39}$$

$$\tilde{\mathbf{x}}_k^{l+1} \leftarrow \arg\min_{\tilde{\mathbf{x}}_k}\left(\lambda_k^l\right)^H\left(\tilde{\mathbf{x}}^{l+1}-\tilde{\mathbf{x}}_k\right) + \frac{\rho_k}{2}\left\|\tilde{\mathbf{x}}^{l+1}-\tilde{\mathbf{x}}_k\right\|^2$$

$$\text{s.t.}\begin{cases}\tilde{\mathbf{x}}_k^H\tilde{\mathbf{A}}_i\tilde{\mathbf{x}}_k \geqslant \gamma_{th}/B_i, & 1\leqslant k\leqslant K\\ \tilde{\mathbf{x}}_k^H\tilde{\mathbf{A}}_{ij}\tilde{\mathbf{x}}_k = \varepsilon_{ij}, & K+1\leqslant k\leqslant K^2\\ \tilde{\mathbf{x}}_{K^2+1}^H\tilde{\mathbf{x}}_{K^2+1}\leqslant P_2^{\max}, & k=K^2+1\end{cases} \tag{40}$$

$$\lambda_k^{l+1} \leftarrow \lambda_k^l + \rho_k\left(\tilde{\mathbf{x}}^{l+1}-\tilde{\mathbf{x}}_k^{l+1}\right) \tag{41}$$

where the problem (43) for each $\tilde{\mathbf{x}}_k$ is a Quadratical Constraint Quadratic Programming-1 (QCQP-1) problem, which is omitted here for brevity and can be solved by the algorithm in [43]. The main steps of the proposed SCSI-based ADMM BF scheme are summarized in Algorithm 1. The convergence of Algorithm 1 is guaranteed by the ADMM theory, which has been proved in special literature [44].

Algorithm 1: The proposed SCSI-based ADMM BF scheme.

Input: $\{\mathbf{A}_i, \gamma_{th}, P_2^{\max}\}$
Initialize a feasible point $\mathbf{x}^0, \mathbf{v}^0, \rho, \lambda^0$ for problem (29), set $t=0$;
Set the stopping criterion δ_1 and δ_2;
while $\left|\mathbf{x}^{t+1}-\mathbf{x}^t\right| \geqslant \delta_1$ **do**
  Initialize a feasible point $\tilde{\mathbf{x}}^0, \tilde{\mathbf{x}}_i^0, \rho_i, \lambda_i^0$ for problem (32), set $l=0$;
  while $\left|\tilde{\mathbf{x}}^{l+1}-\tilde{\mathbf{x}}^l\right| \geqslant \delta_2$ **do**
    Update $\tilde{\mathbf{x}}^{l+1}$ by (39);
    Update $\tilde{\mathbf{x}}_i^{l+1}$ by solving problem (40);
    Update λ_i^{l+1} by (41);
    $l \leftarrow l+1$;
  end
  Update $\mathbf{x}^{t+1} = \tilde{\mathbf{x}}^l$;
  Update $\mathbf{v}^{t+1}$ by solving (33);
  Update λ^{t+1} by (34);
  $t \leftarrow t+1$;
end
Output: $\{\mathbf{x}^t, \mathbf{v}^t, \lambda^t\}$

By now we have designed a new SCSI-based ADMM BF scheme, which could obtain the corresponding BF weight vector to implement SDMA for RF transmission. In the next subsection, we consider a ZF-based suboptimal BF scheme to solve the optimization problem in (29), which can achieve a good balance between the complexity and performance [31].

B. ZF-Based Suboptimal BF Scheme

From the original problem (26), we can observe that the objective term and interference terms are expressed as $P_{2,i}\mu_i\mathbf{w}_i^H\mathbf{A}_i\mathbf{w}_i$ and $\sum_{j=1,j\neq i}^{K}P_{2,j}\mu_i\mathbf{w}_j^H\mathbf{A}_i\mathbf{w}_j$, respectively. Moreover, when the transmit power $P_{2,i}$ is fixed, we can first exploit ZF technique [45] to remove the interference term $\sum_{j=1,j\neq i}^{K}P_{2,j}\mu_i\mathbf{w}_j^H\mathbf{A}_i\mathbf{w}_j$, and then calculate the optimal power allocation to realize the maximal system ESR. In this context, to eliminate the interference between different IoRT devices, while maximize the performance of the IoRT device D_i, the optimization problem to obtain BF vectors is established as

$$\max_{\mathbf{w}_i}\ \mathbf{w}_i^H\mathbf{a}(\theta_i)\mathbf{a}(\theta_i)^H\mathbf{w}_i \quad \text{s.t. } \mathbf{H}_{-i}^H\mathbf{w}_i = \mathbf{0}_{(K-1)\times 1},\ \mathbf{w}_i^H\mathbf{w}_i = 1, \forall i=1,\cdots,K, \tag{42}$$

where $\mathbf{H}_{-i}^H \triangleq [\mathbf{a}(\theta_1),\cdots\mathbf{a}(\theta_{i-1}),\mathbf{a}(\theta_{i+1}),\cdots,\mathbf{a}(\theta_K)]$ with $\mathbf{a}(\theta_i)$ obtained by applying to singular value decomposition (SVD)

This article has been accepted for publication in a future issue of this journal, but has not been fully edited. Content may change prior to final publication. Citation information: DOI 10.1109/JIOT.2022.3170429, IEEE Internet of Things Journal

to the covariance $\mathbf{A}_i = \Omega_i \mathbf{a}(\theta_i)\mathbf{a}(\theta_i)^H$. According to the null-steering BF technique in ASP, we obtain

$$\mathbf{w}_i^Z = \frac{(\mathbf{I}_N - \mathbf{G}_i)\,\mathbf{a}(\theta_i)}{\|(\mathbf{I}_N - \mathbf{G}_i)\,\mathbf{a}(\theta_i)\|}, \tag{43}$$

where $\mathbf{G}_i = \mathbf{H}_{-i}(\mathbf{H}_{-i}^H\mathbf{H}_{-i})^{-1}\mathbf{H}_{-i}^H$ is the orthogonal projection matrix onto $\mathbf{H}_{-i}$. Subsequently, we formulate the optimization problem to calculate $P_{2,i}$, which can be written as

$$\begin{aligned} &\max_{P_{2,i}} R_2 = \sum_{i=1}^{K} \log_2(1 + P_{2,i}\mu_i b_i) \\ &\text{s.t.} \sum_{i=1}^{K} P_{2,i} \leqslant P_2^{\max}, \end{aligned} \tag{44}$$

where $b_i = \Omega_i \mathbf{a}(\theta_i)^H (\mathbf{I}_N - \mathbf{G}_i)\,\mathbf{a}(\theta_i)$. It can be seen that problem (44) is convex over $P_{2,i}$, which can thus be solved using Karush-Kuhn-Tucker (KKT) optimality conditions. The corresponding Lagrangian can be written as

$$L(\lambda_2, P_{2,i}) = \sum_{i=1}^{K} \log_2(1 + P_{2,i}\mu_i b_i) + \lambda_2 \left(\sum_{i=1}^{K} P_{2,i} - P_2^{\max} \right). \tag{45}$$

By differentiating the Lagrangian with respect to $P_{2,i}$ and setting the derivative to zero, we have

$$\frac{\mu_i b_i}{\ln 2\,(1 + P_{2,i}\mu_i b_i)} + \lambda_2 = 0. \tag{46}$$

According to KKT conditions, the optimal power of the IoRT device can be expressed as two cases.

Case 1. $\lambda_2 = 0$ and $\sum_{i=1}^{K} P_{2,i} < P_2^{\max}$, no solution is obtained.

Case 2. $\lambda_2 \neq 0$ and $\sum_{i=1}^{K} P_{2,i} = P_2^{\max}$, the optimal power for the IoRT device can be calculated by

$$P_{2,i}^* = \left[\frac{1}{K} \left(P_2^{\max} + \sum_{i=1}^{K} \frac{1}{\mu_i b_i} \right) - \frac{1}{\mu_i b_i} \right]^+. \tag{47}$$

Until now, we have proposed two different BF schemes to solve the non-convex optimization problem, and conduct SDMA in RF transmission for achieving the maximal ergodic sum rate. It is worth-mentioning that only the knowledge of the statistical CSI is employed and thus no exact CSI is needed at the UAV, which is different from the existing works [23], [24] where perfect CSI is used.

IV. Performance Analysis

This section first provides the statistical characteristics of the FSO and RF channels, and then derives the closed-form expressions of the system ergodic sum rate for the considered network with two BF schemes.

A. Statistical Characteristics of FSO and RF Channels

When EGC scheme is exploited at the UAV, with the help of (15), the PDF of $I_{EGC} = \sum_{q=1}^{M} I_q$ can be expressed as

$$\begin{aligned} f_{I_{EGC}}(x) = &\frac{\left(\frac{\alpha_M\beta_M}{MI_l}\right)^{\frac{\alpha_M+\beta_M}{2}} x^{\frac{\alpha_M+\beta_M}{2}-1}}{\Gamma(\alpha_M)\Gamma(\beta_M)} \times \\ &G_{0,2}^{2,0}\left[\frac{\alpha_M\beta_M x}{MI_l} \middle| \begin{matrix} - \\ \frac{\alpha_M-\beta_M}{2}, -\frac{\alpha_M-\beta_M}{2} \end{matrix} \right], x \geqslant 0, \end{aligned} \tag{48}$$

where $\alpha_M = M\alpha + \varepsilon_M$ and $\beta_M = M\beta$, $\varepsilon_M = (M-1)\frac{-0.127-0.95\alpha-0.0058\beta}{1+0.00124\alpha+0.98\beta}$ being the adjustment parameter. The PDF expression is more general than that of using a single aperture [37]-[39] and more detailed proof of the PDF expression can be found in [46]. According to (2), the PDF of $\gamma_1 = \bar{\gamma}_1 I_{EGC}^2$ can be expressed as

$$\begin{aligned} f_{\gamma_1}(x) = &\frac{\left(\frac{\alpha_M\beta_M}{MI_l}\right)^{\frac{\alpha_M+\beta_M}{2}} x^{\frac{\alpha_M+\beta_M}{4}-1}}{2\Gamma(\alpha_M)\Gamma(\beta_M)\,\bar{\gamma}_1^{\frac{\alpha_M+\beta_M}{4}}} \\ &\times G_{0,2}^{2,0}\left[\frac{\alpha_M\beta_M}{MI_l}\sqrt{\frac{x}{\bar{\gamma}_1}} \middle| \begin{matrix} - \\ \frac{\alpha_M-\beta_M}{2}, -\frac{\alpha_M-\beta_M}{2} \end{matrix} \right]. \end{aligned} \tag{49}$$

Subsequently, after using the output BF vectors calculated by Algorithm 1 as proposed in this paper, the SINR in (4) for the IoRT device D_i can be written as

$$\gamma_{2,i}^A = \frac{\mu_i|\rho_i|^2 \left|\tilde{\mathbf{w}}_i^H \mathbf{a}(\theta_i)\right|^2}{\sum_{j\neq i}^{K} \mu_i|\rho_i|^2 \left|\tilde{\mathbf{w}}_j^H \mathbf{a}(\theta_i)\right|^2 + 1}. \tag{50}$$

By defining $X \triangleq \sum_{j=1}^{K} \mu_i|\rho_i|^2 \left|\tilde{\mathbf{w}}_j^H \mathbf{a}(\theta_i)\right|^2$ and $Y \triangleq \sum_{j=1, j\neq i}^{K} \mu_i|\rho_i|^2 \left|\tilde{\mathbf{w}}_j^H \mathbf{a}(\theta_i)\right|^2$, with the help of (20), the PDF expressions of which can be, respectively, expressed as

$$f_X(x) = \frac{m_i^{m_i} x^{m_i-1}}{(\Lambda_1\Omega_i)^{m_i}\Gamma(m_i)} \exp\left(-\frac{m_i x}{\Lambda_1\Omega_i}\right), \tag{51}$$

and

$$f_Y(y) = \frac{m_i^{m_i} y^{m_i-1}}{(\Lambda_2\Omega_i)^{m_i}\Gamma(m_i)} \exp\left(-\frac{m_i y}{\Lambda_2\Omega_i}\right), \tag{52}$$

where $\Lambda_1 = \sum_{j=1}^{K} \mu_i \left|\tilde{\mathbf{w}}_j^H \mathbf{a}(\theta_i)\right|^2$ and $\Lambda_2 = \sum_{j=1, j\neq i}^{K} \mu_i \left|\tilde{\mathbf{w}}_j^H \mathbf{a}(\theta_i)\right|^2$.

Meanwhile, when ZF-based suboptimal BF scheme is adopted, with the help of (43) and (47), the SINR for the IoRT device D_i is given by

$$\gamma_{2,i}^Z = P_{2,i}^* \mu_i b_i |\rho_i|^2 \triangleq \bar{\gamma}_{2,i}^Z |\rho_i|^2, \tag{53}$$

where $\bar{\gamma}_{2,i}^S = P_{2,i}^* \mu_i b_i$. Thus, using (20), we can express the corresponding PDF of $\gamma_{2,i}^Z$ as

$$f_{\gamma_{2,i}^Z}(x) = \frac{m_i^{m_i} x^{m_i-1}}{\left(\bar{\gamma}_{2,i}^Z \Omega_i\right)^{m_i}\Gamma(m_i)} \exp\left(-\frac{m_i x}{\bar{\gamma}_{2,i}^Z \Omega_i}\right). \tag{54}$$

This article has been accepted for publication in a future issue of this journal, but has not been fully edited. Content may change prior to final publication. Citation information: DOI 10.1109/JIOT.2022.3170429, IEEE Internet of Things Journal

$$R_1 = \frac{\left(\frac{\alpha_M\beta_M}{MI_l}\right)^{\frac{\alpha_M+\beta_M}{2}}}{2(\ln 2)\Gamma(\alpha_M)\Gamma(\beta_M)\bar{\gamma}_1^{\frac{\alpha_M+\beta_M}{4}}} \underbrace{\int_0^\infty x^{\frac{\alpha_M+\beta_M}{4}-1} G_{2,2}^{1,2}\left[x\middle|\begin{matrix}1,1\\1,0\end{matrix}\right] G_{0,2}^{2,0}\left[\frac{\alpha_M\beta_M}{MI_l}\sqrt{\frac{x}{\bar{\gamma}_1}}\middle|\begin{matrix}-\\ \frac{\alpha_M-\beta_M}{2}, -\frac{\alpha_M-\beta_M}{2}\end{matrix}\right] dx}_{J_1}. \quad (57)$$

$$J_1 = \frac{1}{2\pi} G_{2,6}^{6,1}\left[\frac{(\alpha_M\beta_M)^2}{(MI_l)^2 16\bar{\gamma}_1}\middle|\begin{matrix}-\frac{\alpha_M+\beta_M}{4}, 1-\frac{\alpha_M+\beta_M}{4}\\ \frac{\alpha_M-\beta_M}{4}, \frac{\alpha_M-\beta_M}{4}+\frac{1}{2}, -\frac{\alpha_M-\beta_M}{4}, \frac{1}{2}-\frac{\alpha_M-\beta_M}{4}, -\frac{\alpha_M+\beta_M}{4}, -\frac{\alpha_M+\beta_M}{4}\end{matrix}\right]. \quad (58)$$

B. Ergodic Sum Rate

To calculate the system ergodic sum rate expressed as (5), we should derive the analytical expression of R_1 and R_2 separately. First of all, the ergodic rate of the FSO link R_1 is given by

$$R_1 = B_o E\left[\log_2(1+\gamma_1)\right] = B_o \frac{1}{\ln 2}\int_0^\infty \ln(1+x) f_{\gamma_1}(x) dx. \quad (55)$$

For the convenience of derivation, we employ [40, Eq. (11)] and denote $\ln(1+x)$ in terms of Meijer's G-function as

$$\ln(1+x) = G_{2,2}^{1,2}\left[x\middle|\begin{matrix}1,1\\1,0\end{matrix}\right]. \quad (56)$$

By substituting (49) and (56) into (55), it follows as (57) at the top of the page. Then, with the help of [35, (21)], J_1 in (60) can be calculated as (58) at the top of the page. After plugging (58) into (57), one can obtain

$$R_1 = \frac{B_o\left(\frac{\alpha_M\beta_M}{MI_l}\right)^{\frac{\alpha_M+\beta_M}{2}}}{4\pi(\ln 2)\Gamma(\alpha_M)\Gamma(\beta_M)\bar{\gamma}_1^{\frac{\alpha_M+\beta_M}{4}}} G_{2,6}^{6,1}\left[\frac{(\alpha_M\beta_M)^2}{(MI_l)^2 16\bar{\gamma}_1}\middle|\begin{matrix}\Delta_1\\ \Delta_2\end{matrix}\right], \quad (59)$$

where $\Delta_1 = -\frac{\alpha_M+\beta_M}{4}, 1-\frac{\alpha_M+\beta_M}{4}$ and $\Delta_2 = \frac{\alpha_M-\beta_M}{4}, \frac{\alpha_M-\beta_M}{4}+\frac{1}{2}, -\frac{\alpha_M-\beta_M}{4}, \frac{1}{2}-\frac{\alpha_M-\beta_M}{4}, -\frac{\alpha_M+\beta_M}{4}, -\frac{\alpha_M+\beta_M}{4}$.

For RF links, the ergodic rate for the IoRT device D_i in case of SCSI-based ADMM BF scheme can be expressed as

$$\begin{aligned} R_i^A &= E\left[\log_2\left(1+\gamma_i^A\right)\right] = \frac{1}{\ln 2}E\left[\ln\left(\frac{1+X}{1+Y}\right)\right] \\ &= \frac{1}{\ln 2}\left(E\left[\ln(1+X)\right] - E\left[\ln(1+Y)\right]\right). \end{aligned} \quad (60)$$

Using (51), the first term in (60) can be calculated by

$$\begin{aligned} E\left[\ln(1+X)\right] &= \int_0^\infty \ln(1+x) f_X(x) dx \\ &= \frac{m_i^{m_i}}{(\Lambda_1\Omega_i)^{m_i}\Gamma(m_i)}\int_0^\infty \ln(1+x) x^{m_i-1}\exp\left(-\frac{m_i x}{\Lambda_1\Omega_i}\right) dx. \end{aligned} \quad (61)$$

By employing the expression for $\exp(-x)$ in terms of Meijer's G-function from [35] along with (56), we obtain

$$\begin{aligned} E\left[\ln(1+X)\right] &= \frac{m_i^{m_i}}{(\Lambda_1\Omega_i)^{m_i}\Gamma(m_i)} \times \\ &\int_0^\infty x^{m_i-1} G_{2,2}^{1,2}\left[x\middle|\begin{matrix}1,1\\1,0\end{matrix}\right] G_{0,1}^{1,0}\left[\frac{m_i x}{\Lambda_1\Omega_i}\middle|\begin{matrix}-\\0\end{matrix}\right] dx \\ &= \frac{m_i^{m_i}}{(\Lambda_1\Omega_i)^{m_i}\Gamma(m_i)} G_{2,3}^{3,1}\left[\frac{m_i}{\Lambda_1\Omega_i}\middle|\begin{matrix}-m_i, 1-m_i\\0, -m_i, -m_i\end{matrix}\right]. \end{aligned} \quad (62)$$

Similarly, the second term in (60) is given by

$$E\left[\ln(1+Y)\right] = \frac{m_i^{m_i}}{(\Lambda_2\Omega_i)^{m_i}\Gamma(m_i)} G_{2,3}^{3,1}\left[\frac{m_i}{\Lambda_2\Omega_i}\middle|\begin{matrix}-m_i, 1-m_i\\0, -m_i, -m_i\end{matrix}\right]. \quad (63)$$

By substituting (62) and (63) into (60), the ergodic rate R_i^A can be obtained as (64) at the bottom of the page. Thus, according to (7), the ergodic sum rate R_2^A for RF transmission with SCSI-based ADMM BF scheme is given by (65) at the bottom of the page. Finally, by plugging (59) and (65) into (5), the closed-form expression of system ergodic sum rate for the considered network with SCSI-based ADMM BF scheme can be easily obtained.

Based on an analysis similar to the ADMM BF scheme, the ergodic sum rate R_2^Z for RF transmission with ZF-based suboptimal BF scheme can be derived as

$$\begin{aligned} R_2^Z &= B_R\sum_{i=1}^K R_i^Z \\ &= \frac{B_R}{\ln 2}\sum_{k=1}^K \frac{m_i^{m_i}}{\left(\bar{\gamma}_{2,i}^Z\Omega_i\right)^{m_i}\Gamma(m_i)} G_{2,3}^{3,1}\left[\frac{m_i}{\bar{\gamma}_{2,i}^Z\Omega_i}\middle|\begin{matrix}-m_i, 1-m_i\\0, -m_i, -m_i\end{matrix}\right]. \end{aligned} \quad (66)$$

Then, by using (59) and (66) into (5), the closed-form expression of system ergodic sum rate for ZF-based suboptimal BF scheme can be easily obtained.

$$R_i^A = \frac{1}{\ln 2}\frac{m_i^{m_i}}{\Omega_i^{m_i}\Gamma(m_i)}\left(\Lambda_1^{-m_i} G_{2,3}^{3,1}\left[\frac{m_i}{\Lambda_1\Omega_i}\middle|\begin{matrix}-m_i, 1-m_i\\0, -m_i, -m_i\end{matrix}\right] - \Lambda_2^{-m_i} G_{2,3}^{3,1}\left[\frac{m_i}{\Lambda_2\Omega_i}\middle|\begin{matrix}-m_i, 1-m_i\\0, -m_i, -m_i\end{matrix}\right]\right). \quad (64)$$

$$R_2^A = B_R\sum_{i=1}^K R_i^A = \frac{B_R}{\ln 2}\sum_{i=1}^K \frac{m_i^{m_i}}{\Omega_i^{m_i}\Gamma(m_i)}\left(\Lambda_1^{-m_i} G_{2,3}^{3,1}\left[\frac{m_i}{\Lambda_1\Omega_i}\middle|\begin{matrix}-m_i, 1-m_i\\0, -m_i, -m_i\end{matrix}\right] - \Lambda_2^{-m_i} G_{2,3}^{3,1}\left[\frac{m_i}{\Lambda_2\Omega_i}\middle|\begin{matrix}-m_i, 1-m_i\\0, -m_i, -m_i\end{matrix}\right]\right). \quad (65)$$

This article has been accepted for publication in a future issue of this journal, but has not been fully edited. Content may change prior to final publication. Citation information: DOI 10.1109/JIOT.2022.3170429, IEEE Internet of Things Journal

V. Numerical Results

In this section, we provide computer simulations to validate the theoretical analysis and the effectiveness of the proposed BF schemes. Moreover, we investigate the impact of typical system parameters on the performance. Here, we consider that the FSO link experiences weak atmospheric turbulent with $(\alpha, \beta) = (2.902, 2.51)$. For ease of analysis, it is assumed that all the IoRT devices are subject to the same channel conditions, i.e., $m_i = m, \Omega_i = \Omega$. The other parameters are provided in Table I. Here, the satellite transmit power and FSO bandwidth are sufficiently high to support the massive connectivity. Similar to [36] and [39], we first discuss the effect of aperture numbers on satellite backbone network when EGC scheme is adopted or not, as illustrated in Fig. 2. Then, we fix the transmit power at satellite and focus on investigating the ergodic sum rate of the considered network, as illustrated in Figs. 3 to 6. In particular, we take the related works [36] which adopted maximal ratio transmission (MRT) technique to serve multiple users simultaneously as benchmark I, and [39] where the MRT technique and multiuser scheduling were used for RF transmission as benchmark II. For sake of convenience, we call the proposed schemes as "ADMM BF scheme" and "ZF-based BF scheme", respectively.

Table I. System and channel parameters [8][36][39]

FSO Channel Parameters	**Value**
FSO bandwidth	$B_O = 1280$ MHz
FSO wavelength	$\lambda_O = 1550$ nm
Transmitter diameter	$D_t = 0.15$ m
Receiver diameter	$D_r = 0.25$ m
Free-space losses	$A_{FS} = 268$ dB
Atmosphere attention	$A_{ATM} = 0.5$ dB
Lenses losses	$L = 3$ dB
System margin	$M_s = 3$ dB
RF Channel Parameters	**Value**
Operating frequency	$f = 2$ GHz
RF bandwidth	$B_R = 1$ MHz
RF path-loss exponent	$\alpha_l = 2.5$
Height of UAV	H = 1000 m
Radius of IoRT devices area	R = 500 m
Noise temperature	T = 300 K

Fig. 2 depicts the ergodic sum rate of the FSO channel versus the satellite transmit power with different number of apertures. One can see that the analytical results are in a perfect match with Monte Carlo simulations, justifying the validity of the derived closed-form expression of ergodic rate in FSO link. Also, the ergodic sum rate improves sufficiently as the aperture numbers increases, which is benefit from diversity gain.

In Fig. 3, the convergence rate of our proposed SCSI-based ADMM BF scheme is illustrated. By assuming that the number of antennas as $N = 32$, it can be seen that the alogorithm will converge under different UAV transmit power. In addition, as the increasing transmit power, the convergence rate would be a bit faster. This is because the initial feasible points are relevant to the transmit power.

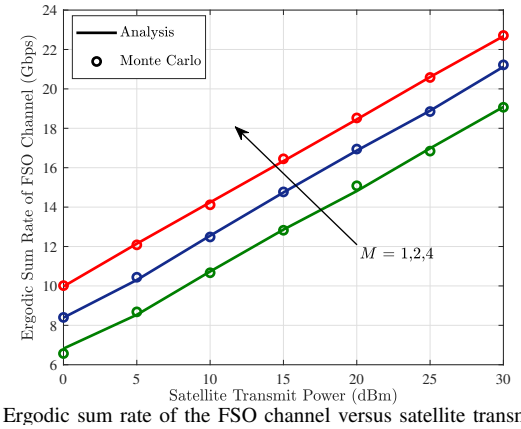

Fig. 2. Ergodic sum rate of the FSO channel versus satellite transmit power.

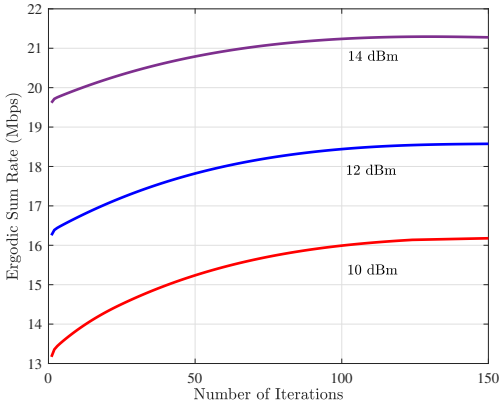

Fig. 3. Ergodic sum rate versus number of iterations under different UAV transmit power.

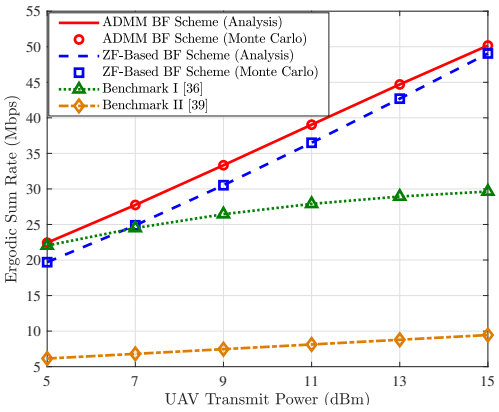

Fig. 4. Ergodic sum rate versus number of IoRT devices.

Under various BF schemes, the ergodic sum rates versus UAV transmit power are plotted in Fig. 4. Here, we set the number of IoRT devices $K = 10$ and antenna number $N = 44$. As we expected, the analytical results match well with simulation results, which verify the correctness of theoretical analysis for the proposed BF schemes. As we see the benchmark II has the worst performance among four schemes, which is because that only one device is served in each time slot. Since the noise dominates over the interferenc at low transmit power, the benchmark I obtain higher ergodic sum rate over ZF-based BF scheme. On the contrary, in high transmit power the interference dominates over the noise, the ZF-based BF scheme

This article has been accepted for publication in a future issue of this journal, but has not been fully edited. Content may change prior to final publication. Citation information: DOI 10.1109/JIOT.2022.3170429, IEEE Internet of Things Journal

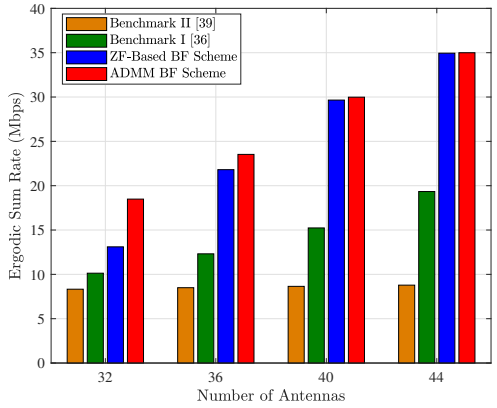

Fig. 5. Ergodic sum rate versus number of antennas.

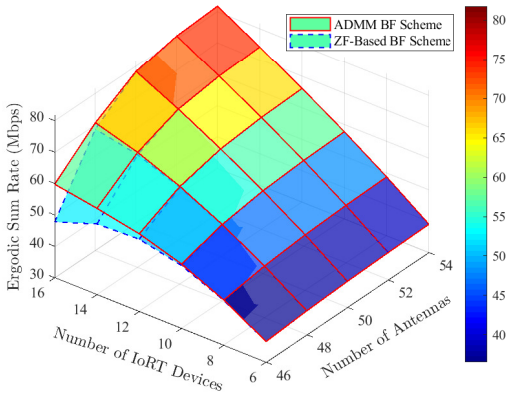

Fig. 6. Ergodic sum rate versus antenna number and IoRT devices number.

can remove the inter-user interference and thus achieving significant performance improvement compared to benchmark I. Moreover, as the transmit power increases, the ergodic sum rate of ZF-based BF scheme is close to ADMM BF scheme.

Fig. 5 depicts the ergodic sum rates versus different antenna numbers when the total transmit power at UAV is set as 10 dBm. Four sets of histograms are plotted. As we can readily observe, increasing the antenna number yields a significant rate improvement in four BF schemes, in particular for ZF-based BF scheme and ADMM BF scheme. Besides, it can be easily noticed that the ZF-based BF scheme has the similar performance to the ADMM BF scheme when the antenna number is large, which is due to the large antenna arrays. From Figs. 4 and 5, we can see that our proposed schemes have the superior performance than the benchmark schemes.

The ergodic sum rates versus antenna and IoRT devices number for two proposed BF schemes are shown in Fig. 6. It can be observed that system performance in terms of ergodic sum rate increases with the antenna and IoRT devices number. Moreover, compared with ADMM BF scheme, the ergodic sum rate for ZF-based BF scheme is lower in the case of large IoRT devices as well as small antenna number, which is due to the limited number of antennas and the higher correlation among large amounts of smart devices.

VI. Conclusion

We have studied the downlink transmission of a satellite and UAV integrated network in IoRT applications, where the satellite FSO links are subject to Gamma-Gamma fading while the UAV RF links are characterized by Nakagami-*m* fading channel. In particular, EGC scheme and SDMA technique have been adopted for FSO communication and RF transmission, respectively. To maximize the ergodic sum rate of the considered network, we have proposed SCSI-based ADMM BF scheme and ZF-based suboptimal BF scheme for RF transmission. Then, closed-form expressions for ESR of the considered network with proposed schemes have been derived. Numerical simulations have been conducted to validate the correctness of the theoretical analysis and effectiveness of two proposed BF schemes. Our proposed schemes and new findings can provide insightful guidance for the design of a satellite and UAV integrated network in IoRT applications.

References

[1] D. Wang, D. Chen, B. Song, N. Guizani, X. Yu, and X. Du, "From IoT to 5G I-IoT: The next generation IoT-based intelligent algorithms and 5G technologies," *IEEE Commun. Mag.*, vol. 56, no. 10, pp. 114–120, Oct. 2018.

[2] Z. Lin, M. Lin, T. de Cola, J.-B. Wang, W.-P. Zhu, and J. Cheng, "Supporting IoT with rate-splitting multiple access in satellite and aerial-integrated networks," *IEEE Internet Things J.*, vol. 8, no. 14, pp. 11 123–11 134, Jul. 2021.

[3] G. A. Akpakwu, B. J. Silva, G. P. Hancke, and A. M. Abu-Mahfouz, "A survey on 5G networks for the internet of things: Communication technologies and challenges," *IEEE Access*, vol. 6, pp. 3619–3647, Feb. 2018.

[4] Y. Wang, Z. Li, Y. Chen, M. Liu, X. Lyu, X. Hou, and J. Wang, "Joint resource allocation and UAV trajectory optimization for space-air-ground internet of remote things networks," *IEEE Syst. J.*, Sept. 2020, to be published, doi:10.1109/JSYST.2020.3019463.

[5] Z. Li, Y. Wang, M. Liu, R. Sun, Y. Chen, J. Yuan, and J. Li, "Energy efficient resource allocation for UAV-assisted space-air-ground internet of remote things networks," *IEEE Access*, vol. 7, pp. 145 348–145 362, Oct. 2019.

[6] M. De Sanctis, E. Cianca, G. Araniti, I. Bisio, and R. Prasad, "Satellite communications supporting internet of remote things," *IEEE Internet Things J.*, vol. 3, no. 1, pp. 113–123, Feb. 2016.

[7] Z. Wang, M. Lin, S. Sun, M. Cheng, and W.-P. Zhu, "Robust beamforming for enhancing user fairness in multibeam satellite systems with NOMA," *IEEE Trans. Veh. Technol.*, vol. 71, no. 1, pp. 1010–1014, Jan. 2022.

[8] Q. Huang, M. Lin, J. Wang, T. A. Tsiftsis, and J. Wang, "Energy efficient beamforming schemes for satellite-aerial-terrestrial networks," *IEEE Trans. Commun.*, vol. 68, no. 6, pp. 3863–3875, June 2020.

[9] Z. Qu, G. Zhang, H. Cao, and J. Xie, "LEO satellite constellation for internet of things," *IEEE Access*, vol. 5, pp. 18 391–18 401, Aug. 2017.

[10] S.-Y. Lien, K.-C. Chen, and Y. Lin, "Toward ubiquitous massive accesses in 3GPP machine-to-machine communications," *IEEE Commun. Mag.*, vol. 49, no. 4, pp. 66–74, Apr. 2011.

[11] B. Li, Z. Fei, and Y. Zhang, "UAV communications for 5G and beyond: Recent advances and future trends," *IEEE Internet Things J.*, vol. 6, no. 2, pp. 2241–2263, Apr. 2019.

[12] X. Huang, J. A. Zhang, R. P. Liu, Y. J. Guo, and L. Hanzo, "Airplane-aided integrated networking for 6G wireless: Will it work?" *IEEE Veh. Technol. Mag.*, vol. 14, no. 3, pp. 84–91, Jul. 2019.

[13] O. Kodheli, E. Lagunas, N. Maturo, S. K. Sharma, B. Shankar, J. F. M. Montoya, J. C. M. Duncan, D. Spano, S. Chatzinotas, S. Kisseleff, J. Querol, L. Lei, T. X. Vu, and G. Goussetis, "Satellite communications in the new space era: A survey and future challenges," *IEEE Commun. Surveys Tuts.*, vol. 23, no. 1, pp. 70–109, 1st quart. 2021.

[14] Y. Zhu, W. Bai, M. Sheng, J. Li, D. Zhou, and Z. Han, "Joint UAV access and GEO satellite backhaul in IoRT networks: Performance analysis and optimization," *IEEE Internet Things J.*, vol. 8, no. 9, pp. 7126–7139, May 2021.

[15] H. Kaushal and G. Kaddoum, "Optical communication in space: Challenges and mitigation techniques," *IEEE Commun. Surveys Tuts.*, vol. 19, no. 1, pp. 57–96, 1st quart. 2017.

[16] Q. Huang, M. Lin, W.-P. Zhu, S. Chatzinotas, and M.-S. Alouini, "Performance analysis of integrated satellite-terrestrial multiantenna relay networks with multiuser scheduling," *IEEE Trans. Aerosp. Electron. Syst.*, vol. 56, no. 4, pp. 2718–2731, Aug. 2020.

[17] H. Kong, M. Lin, J. Zhang, J. Ouyang, J.-B. Wang, and P. K. Upadhyay, "Ergodic sum rate for uplink NOMA transmission in satellite-aerial-ground integrated networks," *Chinese J. Aeronaut.*, 2021, to be published, doi: 10.1016/j.cja.2021.10.039.

[18] S. Cluzel, L. Franck, J. Radzik, S. Cazalens, M. Dervin, C. Baudoin, and D. Dragomirescu, "3GPP NB-IoT coverage extension using LEO satellites," in *2018 IEEE 87th Veh. Technol. Conf. (VTC Spring)*, June 2018, pp. 1–5.

[19] G. Giambene, E. O. Addo, and S. Kota, "5G aerial component for IoT support in remote rural areas," in *2019 IEEE 2nd 5G World Forum (5GWF)*, Oct. 2019, pp. 572–577.

[20] T. Hou, Y. Liu, Z. Song, X. Sun, and Y. Chen, "Multiple antenna aided NOMA in UAV networks: A stochastic geometry approach," *IEEE Trans. Commun.*, vol. 67, no. 2, pp. 1031–1044, Feb. 2019.

[21] Y. Zeng, R. Zhang, and T. J. Lim, "Throughput maximization for UAV-enabled mobile relaying systems," *IEEE Trans. Commun.*, vol. 64, no. 12, pp. 4983–4996, Dec. 2016.

[22] L. Liu, S. Zhang, and R. Zhang, "Multi-beam UAV communication in cellular uplink: Cooperative interference cancellation and sum-rate maximization," *IEEE Trans. Wireless Commun.*, vol. 18, no. 10, pp. 4679–4691, Oct. 2019.

[23] G. Pan, J. Ye, Y. Zhang, and M.-S. Alouini, "Performance analysis and optimization of cooperative satellite-aerial-terrestrial systems," *IEEE Trans. Wireless Commun.*, vol. 19, no. 10, pp. 6693–6707, Oct. 2020.

[24] P. K. Sharma, D. Deepthi, and D. I. Kim, "Outage probability of 3-D mobile uav relaying for hybrid satellite-terrestrial networks," *IEEE Commun. Lett.*, vol. 24, no. 2, pp. 418–422, Feb. 2020.

[25] X. Liu, M. Lin, Q. Huang, J. Wang, and J. Ouyang, "Performance analysis for multi-user integrated satellite and UAV cooperative networks," *Physical Commun.*, vol. 36, p. 100762, Oct. 2019.

[26] F. Qi, X. Zhu, G. Mang, M. Kadoch, and W. Li, "UAV network and IoT in the sky for future smart cities," *IEEE Netw.*, vol. 33, no. 2, pp. 96–101, Feb. 2019.

[27] B. Bag, A. Das, and A. Chandra, "Capacity analysis for Rayleigh/gamma-gamma mixed RF/FSO relayed transmission," in *2017 Int. Conf. on Wireless Commun., Signal Process. and Netw. (WiSPNET)*, Mar. 2017, pp. 1828–1832.

[28] M. Li, Y. Hong, C. Zeng, Y. Song, and X. Zhang, "Investigation on the UAV-to-satellite optical communication systems," *IEEE J. Sel. Areas Commun.*, vol. 36, no. 9, pp. 2128–2138, Sept. 2018.

[29] M. Antonini, S. Betti, V. Carrozzo, E. Duca, and M. Ruggieri, "Feasibility analysis of a HAP-LEO optical link for data relay purposes," in *proc. 2006 IEEE Aerosp. Conf.*, Mar. 2006, pp. 1–7.

[30] E. Illi, F. El Bouanani, F. Ayoub, and M.-S. Alouini, "A PHY layer security analysis of a hybrid high throughput satellite with an optical feeder link," *IEEE Open J. Commun. Soc.*, vol. 1, pp. 713–731, June 2020.

[31] E. Zedini, A. Kammoun, and M.-S. Alouini, "Performance of multibeam very high throughput satellite systems based on FSO feeder links with HPA nonlinearity," *IEEE Trans. Wireless Commun.*, vol. 19, no. 9, pp. 5908–5923, Sept. 2020.

[32] M. R. Bhatnagar and M. K. Arti, "Performance analysis of hybrid satellite-terrestrial FSO cooperative system," *IEEE Photon. Technol. Lett.*, vol. 25, no. 22, pp. 2197–2200, Nov. 2013.

[33] M. I. Petkovic, G. T. Djordjevic, and Z. M. Marjanovic, "Analytical approach in evaluation of outage probability of DF based hybrid satellite-terrestrial FSO cooperative system," in *Proc. the 13th TELSIKS*, Oct. 2017, pp. 326–329.

[34] A. M. Salhab, F. S. Al-Qahtani, R. M. Radaydeh, S. A. Zummo, and H. Alnuweiri, "Power allocation and performance of multiuser mixed RF/FSO relay networks with opportunistic scheduling and outdated channel information," *J. Lightw. Technol.*, vol. 34, no. 13, pp. 3259–3272, Jul. 2016.

[35] E. Zedini, H. Soury, and M.-S. Alouini, "On the performance analysis of dual-hop mixed FSO/RF systems," *IEEE Trans. Wireless Commun.*, vol. 15, no. 5, pp. 3679–3689, 2016.

[36] H. Ajam, M. Najafi, V. Jamali, and R. Schober, "Ergodic sum rate analysis of UAV-based relay networks with mixed RF-FSO channels," *IEEE Open J. Commun. Soc.*, vol. 1, pp. 164–178, Feb. 2020.

[37] H. Kong, M. Lin, W.-P. Zhu, H. Amindavar, and M.-S. Alouini, "Multiuser scheduling for asymmetric FSO/RF links in satellite-UAV-terrestrial networks," *IEEE Wireless Commun. Lett.*, vol. 9, no. 8, pp. 1235–1239, Aug. 2020.

[38] Q. Huang, M. Lin, W.-P. Zhu, J. Cheng, and M.-S. Alouini, "Uplink massive access in mixed RF/FSO satellite-aerial-terrestrial networks," *IEEE Trans. Commun.*, vol. 69, no. 4, pp. 2413–2426, Apr. 2021.

[39] P. K. Singya and M.-S. Alouini, "Performance of UAV assisted multiuser terrestrial-satellite communication system over mixed FSO/RF channels," *IEEE Trans. Aerosp. Electron. Syst.*, Sept. 2021, to be published, doi: 10.1109/TAES.2021.3111787.

[40] V. Adamchik and O. Marichev, "The algorithm for calculating integrals of hypergeometric type functions and its realization in reduce system," in *Proc. the Int. Symp. on Symbolic and Algebr. Computation*. ACM, 1990, pp. 212–224.

[41] A. A. Khuwaja, Y. Chen, N. Zhao, M.-S. Alouini, and P. Dobbins, "A survey of channel modeling for UAV communications," *IEEE Commun. Surveys Tuts.*, vol. 20, no. 4, pp. 2804–2821, 4th quart. 2018.

[42] M. Lin, Z. Lin, W.-P. Zhu, and J. Wang, "Joint beamforming for secure communication in cognitive satellite terrestrial networks," *IEEE J. Sel. Areas Commun.*, vol. 36, no. 5, pp. 1017–1029, May 2018.

[43] K. Huang and N. D. Sidiropoulos, "Consensus-ADMM for general quadratically constrained quadratic programming," *IEEE Trans. Signal Process.*, vol. 64, no. 20, pp. 5297–5310, Oct. 2016.

[44] M. Hong, Z.-Q. Luo, and M. Razaviyayn, "Convergence analysis of alternating direction method of multipliers for a family of nonconvex problems," *SIAM Journal on Optimization*, vol. 26, no. 1, pp. 337–364, Jan. 2016.

[45] E. Björnson, M. Bengtsson, and B. Ottersten, "Optimal multiuser transmit beamforming: A difficult problem with a simple solution structure," *IEEE Signal Process. Mag.*, vol. 31, no. 4, pp. 142–148, Jul. 2014.

[46] N. D. Chatzidiamantis and G. K. Karagiannidis, "On the distribution of the sum of Gamma-Gamma variates and applications in RF and optical wireless communications," *IEEE Trans. Commun.*, vol. 59, no. 5, pp. 1298–1308, May 2011.